MODELING AND ANALYSIS OF ABSORPTION PERFORMANCE OF UNDERWATER ANECHOIC LAYERS WITH CAVITIES

Trinh Van Hai [1*], Nguyen Thien Van[2]

Abstract: *Anechoic layer is vital for the underwater acoustic stealth of submarines. This paper develops a simulation-based model for analysis of the acoustic properties of an underwater anechoic layer containing air-filled cavities. First, we present a numerical framework at a relevant scale to implement the acoustical model of an anechoic coating. Then, an investigation of the effects of cavity geometry and elastic property of matrix materials on the absorption property of the anechoic layer is conducted after a validation step. It can be stated from the obtained results that we enable to improve the absorption performance of the considered anechoic coating by tuning its structural factors and mechanical characteristics.*

Keywords: Anechoic layer; Periodic cavity; Local structure; Unit cell; Absorption performance.

1. INTRODUCTION

Submarines are often covered with resonant sound absorbers known as anechoic coatings or tiles in order to avoid detection by sonar. The complicated multicomponent and multi-scale structures are used for a high-quality acoustic stealth. By considering their microstructure, these anechoic structures can be categorized: air-filled cavity, multi-layer composite, and pressure-resisting [1]. Anechoic layer based on air-filled cavities, two types of resonance mechanisms due to the radial motion of the hole wall and the drum-like oscillations of the cover layer [2]. In addition, the developed structure allows broadening and tailoring its acoustic performance by tuning geometric parameters of the distribution of cavities. The macroscopic acoustic properties are highly dependent on the local microstructural features of each individual layers as well as the layer configuration [3].

In order to characterize the link between the microstructural parameters of anechoic structures and their overall acoustic performance, different approaches have been proposed such as analytical [4-6], numerical [7-10], and experimental methods [11, 12]. A number of analytical studies addresses structure-acoustic problems using the transfer matrix method or effective medium models. However, these analytical models often make simplifications on the displacement field and geometry, thereby imposing limitations on the type of problems to be solved as well as structures applied. On contract, the numerical approach such as finite element method (FEM) is more flexible in dealing with complex structures which allows analyzing harmonic wave propagation in single- or multi-layered viscoelastic gratings with periodic or random structures. In this paper, a finite element–based model scheme is developed for modeling and analysis of the acoustic properties of anechoic structures having matrix viscoelastic materials within air-filled cavities.

2. MODELING ANECHOIC LAYER

2.1. Governing equations for structure-acoustic analysis

The structure-acoustic system consists of a fluid domain, Ω_f, a solid domain, Ω_s, and the solid-fluid interface, $\partial\Omega$ (figure 1). In three-dimensional space, the governing equations and boundary conditions of this system can be written [13, 14]:

$$\sum_{j=1}^{3}\frac{\partial}{\partial x_j}\left(\sum_{l=1}^{3}\sum_{k=1}^{3}c_{ijkl}\frac{\partial^2 u_{si}}{\partial^2 t}\right)=\rho_s\frac{\partial^2 u_{si}}{\partial^2 t}\quad (i=1,2,3)\ \text{ in }\ \Omega_s, \tag{1}$$

$$\frac{\partial^2 p}{\partial^2 t}-c_0^2\nabla^2 p=c_0^2\frac{\partial q_f}{\partial t}\quad \text{in}\ \Omega_f\ , \tag{2}$$

$$\boldsymbol{u}_s\cdot\boldsymbol{n}=\boldsymbol{u}_f\cdot\boldsymbol{n}\ \text{ and }\ \boldsymbol{S}_s=-p\boldsymbol{I}_3\quad \text{on}\ \partial\Omega, \tag{3}$$

Where: t is the time variable; u_{si} (i = 1,2,3) are three component of the displacement $\boldsymbol{u}_s$; c_{ijkl} (i,j,l,k = 1,2,3) are the elastic constants of stiffness tensor $\boldsymbol{C}$; ρ_s represents the density of the solid; x_j represent the coordinate variable x, y and z respectively; p is the dynamic pressure related with the dynamic density ρ_f by the constitutive condition $p=c_0^2\rho_f$ with q_f is the added fluid mass per unit volume and c_0 is the speed of sound; $\boldsymbol{u}_f$ is the displacement in fluid linked with the pressure as $\nabla p=-\rho_0\,\partial^2\boldsymbol{u}_f/\partial^2 t$ with ρ_0 is the static density of air, and n is the normal direction of the boundary; $\boldsymbol{I}_3$ is a 3×3 unitary matrix; $\boldsymbol{S}_s$ is the Cauchy stress tensor. Noted that the components of stress tensor are estimated from stress vector $\boldsymbol{\sigma}_s\left(=\boldsymbol{C}:\boldsymbol{\varepsilon}_s\right)$. The strain vector $\boldsymbol{\varepsilon}_s$ is deduced from the strain-displacement relation as $\boldsymbol{\varepsilon}_s=\tilde{\nabla}\boldsymbol{u}_s$. The differential operators ∇ and $\tilde{\nabla}$ are introduced as:

$$\nabla=\left[\partial/\partial x_1\quad \partial/\partial x_2\quad \partial/\partial x_3\right]^T \tag{4a}$$

$$\tilde{\nabla}=\begin{bmatrix}\partial/\partial x_1 & 0 & 0 & \partial/\partial x_2 & \partial/\partial x_3 & 0\\ 0 & \partial/\partial x_2 & 0 & \partial/\partial x_1 & 0 & \partial/\partial x_3\\ 0 & 0 & \partial/\partial x_3 & 0 & \partial/\partial x_1 & \partial/\partial x_2\end{bmatrix}^{\mathrm{T}}. \tag{4b}$$

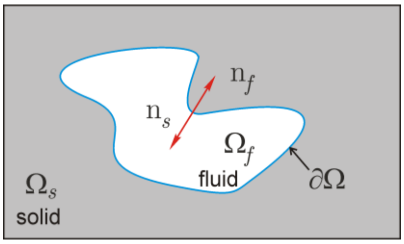

Figure 1. *Schematic diagram of acoustic fluid-structure interaction.*

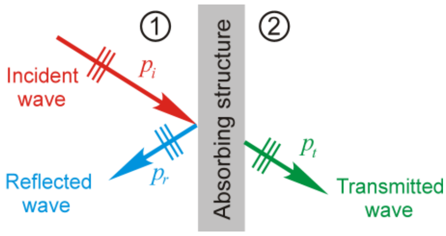

Figure 2. *Diagram of an acoustic material layer excited by an acoustic wave.*

Based on the above governing equations and boundary conditions, using the FEM schematic, the discretized form of the governing equation for the coupled structure-acoustic problem can be written in matrix form as follows [13, 15]:

$$\begin{bmatrix}\boldsymbol{M}_s & 0\\ \rho_0 c_0\boldsymbol{H}^{\mathrm{T}} & \boldsymbol{M}_f\end{bmatrix}\begin{bmatrix}\ddot{\boldsymbol{u}}_s\\ \ddot{\boldsymbol{p}}_f\end{bmatrix}+\begin{bmatrix}\boldsymbol{K}_s & -\boldsymbol{H}\\ 0 & \boldsymbol{K}_f\end{bmatrix}\begin{bmatrix}\boldsymbol{u}_s\\ \boldsymbol{p}_f\end{bmatrix}=\begin{bmatrix}\boldsymbol{f}_s\\ \boldsymbol{f}_f\end{bmatrix}, \tag{5}$$

Where: $\boldsymbol{M}$, $\boldsymbol{C}$ and $\boldsymbol{K}$ are the global mass, damping, and stiffness matrices, respectively; The subscripts '*s*' and '*f*' denote the solid and the fluid domains, respectively; $\boldsymbol{u}_s$ is the nodal displacement vector in the structural domain; $\boldsymbol{p}_f$ is the nodal pressure vector in the acoustic domain; $\boldsymbol{f}_s$ and $\boldsymbol{f}_f$ are the nodal structural force and the nodal acoustic pressure vectors, respectively.

2.2. Unit cell modeling and parameter calculation

In acoustics, complex form is often used for representing the sound waves and the harmonic wave is depicted at frequency ω and wave number k as [9, 15]:

$$p_0(t,\boldsymbol{x}) = A_0 \exp[j(\omega t - k\boldsymbol{x} - \phi_0)], \tag{6}$$

Where: A_0 is the amplitude; ϕ_0 is the initial phase; j is the imaginary unit.

It can be known that when interacting with the material or object surface, the sound wave may be absorbed, transmitted and reflected. Therefore, the incident wave energy would be partly separated into three corresponding components (see figure 2 and figure 3a).

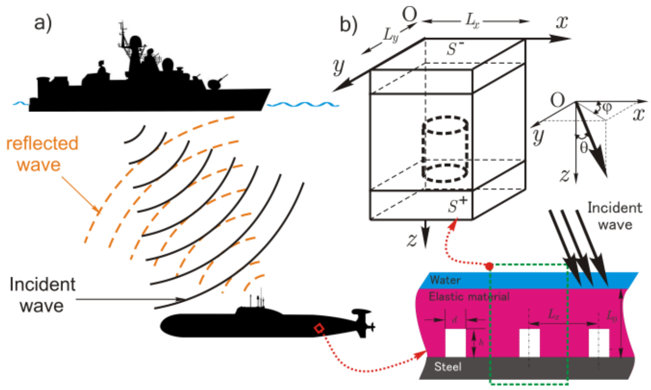

Figure 3. *A submarine under detection by the active sonar (a) and its anechoic structure with a viscoelastic material backing steel hull and a description of the unit cell (b).*

The structure is excited by a harmonic plane wave from the semi-infinite fluid medium. The expression of the incident wave is:

$$p_{\text{in}}(x,y,z) = \exp\left[-jk\left(x\sin\theta\cos\varphi + y\sin\theta\cos\varphi + z\cos\theta\right)\right], \tag{7}$$

Where the time dependence exp(-$j\omega t$) as shown in Eq. (6) has been omitted for clarity, θ and φ denote the direction of the incident wave (see figure 3b).

According to Bloch's theorem, if the structure has the periodic distance L_x in the x direction and L_y in the y direction, any space function χ (e.g., pressure, displacement) satisfies the following relation [9, 16]:

$$\chi\left(x+L_x, y+L_y, z\right) = \chi\left(x,y,z\right)\exp\left(jL_x k\sin\theta\cos\varphi\right)\exp\left(jL_y k\sin\theta\sin\varphi\right). \tag{8}$$

Figure 3b shows the unit cell, where S^- and S^+ surfaces parallel to the xOy plane limit the finite element mesh from the half infinite backing and water domains for incidence, respectively. The incident wave and the reflected wave in the domain below the S^- surface and the transmitted wave in the domain above the S^+ surface are given [17]:

$$
\begin{aligned}
p^{-}(x,y,z) &= p_{\text{in}}(x,y,z) + p_r(x,y,z) \\
&= p_{\text{in}}(x,y,z) + \sum_{m,n=-\infty}^{+\infty} R_{mn} \exp\left[-j\left(k_{nmx}x + k_{ny}y - k_{mn}z\right)\right], \\
p^{+}(x,y,z) &= p_t(x,y,z) = \sum_{m,n=-\infty}^{+\infty} T_{mn} \exp\left[j\left(k_{mx}x + k_{ny}y + k_{mn}z\right)\right],
\end{aligned}
\tag{9}
$$

Where:

- R_{mn} and T_{mn} are the reflection and transmission coefficients corresponding to the (m, n)th mode;
- $k_{mx} = 2m\pi/L_x + k\sin\theta\cos\varphi$;
- $k_{ny} = 2n\pi/L_y + k\sin\theta\sin\varphi$;
- $k_{mn}^2 = k^2 - k_{mx}^2 - k_{ny}^2$.

By solving Eq. (5), the nodal values of the pressure on the incident surface (p^-) and transmission surface (p^+) can be obtained. Thus, the unknown coefficient R_{mn} and T_{mn} are can be deduced from two sets of equations establishing based on the number of known pressure values in the corresponding surfaces. It can be noted that each unknown coefficient requires one nodal pressure value. Thus, the anechoic performance as the absorption coefficient (α) can be calculated by [9, 16, 17]:

$$
\alpha = 1 - |R|^2 - |T|^2, \text{ with } R = \sqrt{\sum_{k_{mn}^2>0} |R_{mn}|^2} \text{ and } T = \sqrt{\sum_{k_{mn}^2>0} |T_{mn}|^2} \tag{10}
$$

3. RESULTS AND DISCUSSION

For validation purpose, our modeling is compared with the analytical model and the FEM result for a configuration of an anechoic layer proposed in Ref. [18]. This anechoic tile is structured with a soft elastic layer having an array of a cylindrical cavity (d = 6 mm, h = 40 mm) with $L_x = L_y$ = 30 mm and backing by a steel layer. The material parameters of the elastic and steel layers are listed in table 1. The good agreement obtained shown in figure 4 validates our FEM model. Noted that our simulations are performed with COMSOL Multiphysics v5.3, and the reference data is taken from figure 8.b in [18].

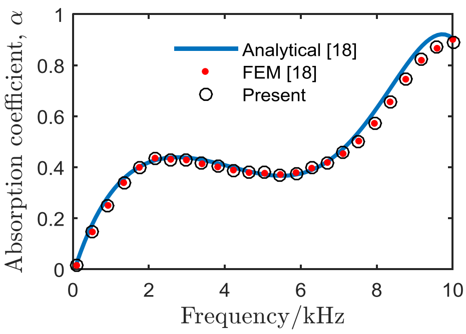

Figure 4. *Comparison of absorption coefficients for validation of the proposed FEM.*

Table 1. *Parameters of materials*

Parameters	Steel hull [11]	Viscoelastic layer [18]
Young's modulus, GPa	216	0.14
Density, kg/m^3	7800	1100
Poisson ratio	0.30	0.49

Next, we investigate the effects of cavity geometry (d, h) and elastic property of matrix materials (Young's modulus, E_r) on the absorption property of anechoic layers. Herein, for all computations, we keep the thickness of the anechoic layer as L_0 = 50 mm, and the lengths of cavity distribution, $L_x = L_y$ = 30 mm. In general, as shown in figure 5, both cavity geometry (i.e., high and diameter) and Young's modulus of elastic material have strong effects on the absorption performance of anechoic layers. It can be noted that in each sub-figure, we calculate for 5 different diameters of the cylindrical cavity, d = 2/4/6/8/10 mm (the thicker lines represent the higher values of d).

Specifically, with h = 40 mm, the anechoic layers with cavities for both values of Young's modulus E_{r1} and E_{r2} provide a high capability of absorption in the high frequency range (e.g., f > 6 kHz, see figure 5 a,c). By reducing the diameter d to 2 mm, the absorption coefficient α increases to a higher value around 0.75 in a larger range of frequency from 3.4 kHz to 10 kHz (figure 5.c).

For h = 20 mm, the matrix material E_{r1} shows poorly the acoustic absorption with α <0.6 over the whole frequency (figure 5.b). In contrast, the anechoic layers made of the matrix material E_{r2} show a better performance (e.g., α > 0.7) of sound incident wave in frequencies from 2.85 kHz to 5.35 kHz, and all considered diameters of cavities have the same first peak with nearly the perfect absorbing capability, $\alpha \sim$ 1.0, at around 3.85 kHz, exception of d = 2 mm (see figure 5.d).

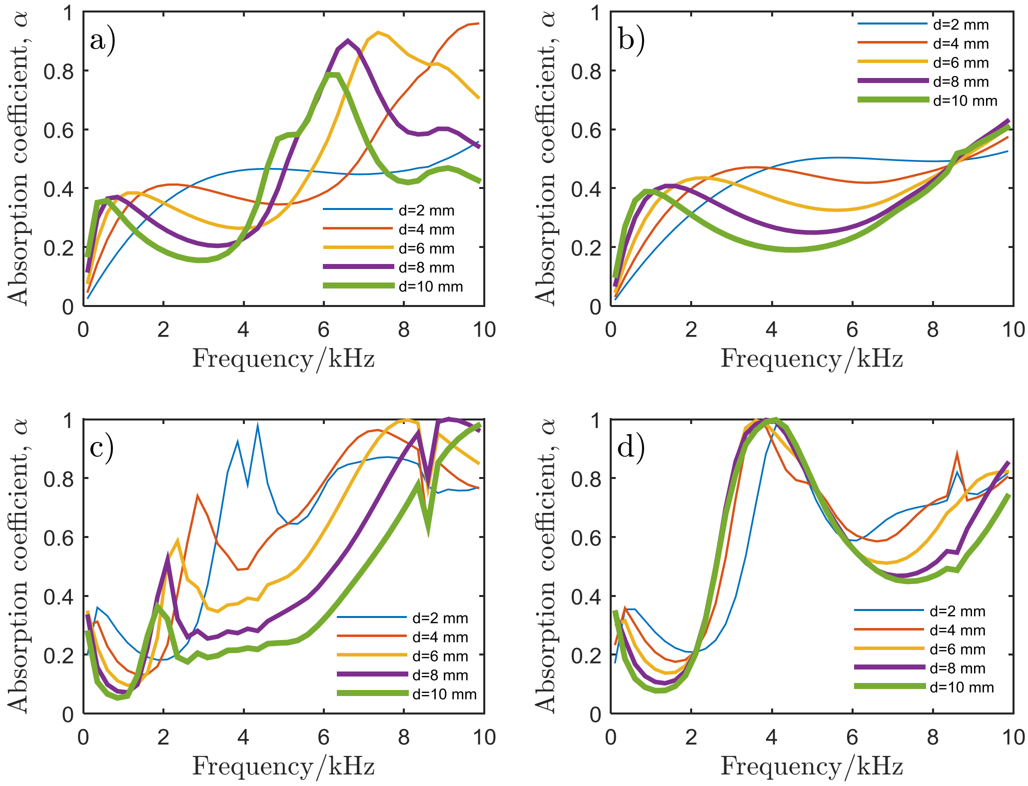

Figure 5. *Effects of cavity geometry ((a,c) for h = 40 mm, and (b,d) for h = 20 mm) and Young modulus of viscoelastic material ((a,b) for E_{r1} = 0.14 GPa, and (c,d) for E_{r2} = 0.014 GPa) on absorption performance of anechoic layers.*

4. CONCLUSIONS

In this work, a numerical approach is presented to investigate the link between microstructure and absorption performance of an anechoic structure having periodic cavities. Very good agreement is observed between the present numerical results with the reference data, which validates the proposed finite element procedure. From investigated results, it is seen that both cavity geometry (i.e., high and diameter of cavities) and elastic properties (i.e., Young's modulus) have strong effects on absorption performance of anechoic layers. With a 40 mm-thick anechoic layer, the softer matrix materials are used the higher absorption property is achieved. In addition, in order to design anechoic layers for low-frequency applications, we need to reduce both the high of cavities and the Young's modulus of the matrix.

Acknowlegdements: *This work is funded by Vietnam National Foundation for Science and Technology Development (NAFOSTED) under Grant No. 107.01-2019.316.*

REFERENCES

[1]. Qian, C. and Y. Li (2017). *"Review on Multi-scale Structural Design of Submarine Stealth Composite"*. DEStech Transactions on Engineering and Technology Research.

[2]. Gaunaurd, G. (1985). "*Comments on 'Absorption mechanisms for waterborne sound in Alberich anechoic layers'"*. Ultrasonics **23**(2): p. 90-91.

[3]. Yang, M. and P. Sheng (2017). *"Sound absorption structures: From porous media to acoustic metamaterials"*. Annual Review of Materials Research 47: p. 3-114.

[4]. Gaunaurd, G., (1977). *"One‐ dimensional model for acoustic absorption in a viscoelastic medium containing short cylindrical cavities"*. The Journal of the Acoustical Society of America. **62**(2): p. 298-307.

[5]. Meng, T., (2014). *"Simplified model for predicting acoustic performance of an underwater sound absorption coating"*. Journal of Vibration and Control. **20**(3): p. 339-354.

[6]. Leroy, V., et al., (2009). *"Transmission of ultrasound through a single layer of bubbles"*. The European Physical Journal E. **29**(1): p. 123-130.

[7]. Sharma, G.S., et al., (2017). *"Acoustic performance of gratings of cylindrical voids in a soft elastic medium with a steel backing"*. The Journal of the Acoustical Society of America. **141**(6): p. 4694-4704.

[8]. Ma, T.-C. et al., (1980). *"Harmonic wave propagation in an infinite elastic medium with a periodic array of cylindrical pores"*. Journal of Sound and Vibration. **71**(4): p. 473-482.

[9]. Hladky- Hennion et al., (1991). *"Analysis of the scattering of a plane acoustic wave by a doubly periodic structure using the finite element method: Application to Alberich anechoic coatings"*. The Journal of the Acoustical Society of America. **90**(6): p. 3356-3367.

[10]. Sohrabi, S.H. and M.J. Ketabdari, (2018). *"Numerical simulation of a viscoelastic sound absorbent coating with a doubly periodic array of cavities"*. Cogent Engineering. **5**(1): p. 1-21.

[11]. Leroy, V., et al., (2015). *"Superabsorption of acoustic waves with bubble metascreens"*. Physical Review B. **91**(2): p. 020301.
[12]. Leroy, V., et al., (2009). *"Design and characterization of bubble phononic crystals"*. Applied Physics Letters. **95**(17): p. 171904.
[13]. Sandberg, G., et al., (2008). *"Fundamentals of fluid-structure interaction"*. Computational aspects of structural acoustics and vibration, Springer. p. 23-101.
[14]. Easwaran, V., & Munjal, M. L. (1993). *"Analysis of reflection characteristics of a normal incidence plane wave on resonant sound absorbers: A finite element approach"*. The Journal of the Acoustical Society of America, *93*(3), p. 1308-1318.
[15]. Hopkins, C. (2012). *"Sound insulation"*. Routledge.
[16]. Fu, X., et al., (2015). *"Sound absorption of a rib-stiffened plate covered by anechoic coatings"*. The Journal of the Acoustical Society of America **137**(3): p. 1551-1556.
[17]. Wen, J., et al., (2011). "*Effects of locally resonant modes on underwater sound absorption in viscoelastic materials"*. The Journal of the Acoustical Society of America **130**(3): p. 1201-1208.
[18]. Ye, C., et al., (2018). *"Influence of hole shape on sound absorption of underwater anechoic layers"*. Journal of Sound and Vibration, 426, p. 54-74.

TÓM TẮT

MÔ HÌNH HÓA VÀ PHÂN TÍCH HIỆU QUẢ HẤP THỤ ÂM CỦA LỚP VỎ TIÊU ÂM VỚI CẤU TRÚC KHOANG KHÍ

Lớp không phản xạ rất quan trọng đối với khả năng tàng hình dưới nước của tàu ngầm. Bài báo này phát triển mô hình dựa trên mô phỏng số để phân tích các đặc tính âm của lớp không phản xạ dưới nước có chứa các khoang khí. Đầu tiên, chúng tôi trình bày mô hình số của lớp vỏ không phản xạ ở cấp độ phù hợp. Sau đó, tiến hành khảo sát ảnh hưởng của hình học khoang khí và tính chất đàn hồi của vật liệu nền đến tính chất hấp thụ của lớp không phản xạ sau khi kiểm chứng mô hình. Từ các kết quả thu được thấy rằng, chúng ta có thể cải thiện hiệu suất hấp thụ của lớp vỏ không phản xạ bằng cách điều chỉnh các yếu tố cấu trúc và đặc tính cơ học.

Từ khóa: Ngói tiêu âm; Khoang khí phân bố tuần hoàn; Cấu trúc cơ sở; Phần tử cơ sở; Đặc tính hấp thụ.

Received 10th October 2020
Revised 5th November 2020
Accepted 10th May 2021

Author affiliations:
[1] Le Quy Don Technical University;
[2] Academy of Military Science and Technology.
*Corresponding author: hai.tv@lqdtu.edu.edu.vn.